

Viewer for an Integral 3D imaging system

Author: Iván Córdoba Oliver

Advisor: Dr. Artur Carnicer Gonzalez

Facultat de Física, Universitat de Barcelona, Diagonal 645, 08028 Barcelona, Spain.*

Abstract: In this work, we study a technique called Integral imaging. This technique consists in a three-dimensional scene reconstruction from two-dimensional images called elementary images. The method we use shows that under natural light conditions and through a computer program, we can get the different planes' depth of the three-dimensional scene. In addition, it will be demonstrated the different objects occlusions that may occur and its effects or problems can be reduced or solved by vertical and horizontal parallax.

I. INTRODUCTION

The main objective of this work is to understand the concept of Integral Imaging (InI). The Integral Imaging is a three-dimensional (3D) image technique that shows us an auto stereoscopic image; that is, such technique brings us the visualization of 3D images without using additional instruments (like glasses). Neither with any specific light conditions since it uses conditions of natural light, which is incoherent light. This technique has evolved since, in 1908, Lippmann proposed a model based on the Integral photography (IP) to record 3D information in a photographic film [1-2].

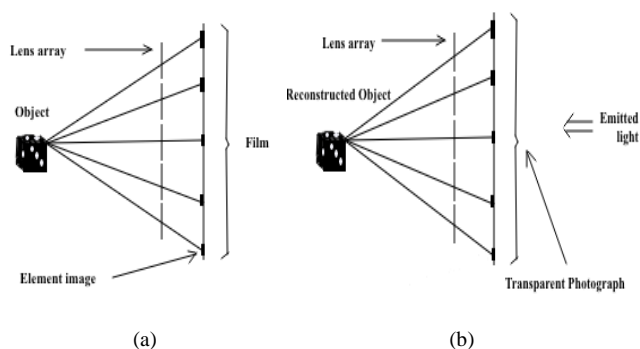


FIG 1. Conventional Integral Photography (IP). (a) Pickup. (b) Reconstruction.

We may find several techniques face to a stereoscopic vision; systems that use an array of lenses or parallax barriers, volumetric systems, holography [7] and the Integral imaging technique [6-7]. It is necessary to comment that the holography is the technique that performs a better 3D sensation, since it registers amplitude and phase of the emitted light of the object, although it has certain limitations since coherent light and stable mechanical systems are required [8-9]. The human vision system has the ability to perceive the depth of the objects through binocular disparity, since the two eyes observe the same scene with differing viewpoints due to the separation between them. Therefore, the brain interprets these position differences creating a feeling of depth. This ability is called stereoscopic vision

and relies on physiological mechanisms such as accommodation, convergence and parallax [6].

With the Integral Image system, we be able to produce this same effect through the capture of elementary images. These elementary images are obtained through a set of micro-lenses or a matrix of sensors with a relative displacement between them. We can even use a single camera capture our elementary images independently [6].

There is a variety of methods for reconstructing a 3D scene. One of the methods, as said before, is to use a set of micro-lenses despite in this work, we will use a single camera system with a CMOS sensor to obtain the set of elementary images. Later, we will use a computational method to achieve the 3D reconstruction [3-4-5].

The InI technique we study in this work, is only based on the Integral imaging computational reconstruction under conditions of natural light. Although, we know several factors that we could take into account when working with this technique, such as, the polarization of light emitted by the different objects or the number of photons recorded by each pixel [4-11]. These factors may influence the InI computational reconstruction.

For a better understanding on how this technique works, we need to understand the concept of irradiance distribution of an image as well [10]. This comprehension of the irradiance distribution is fundamental to understand how the different 3D scene planes are reconstructed since, as we will see later, it depends on the choice of certain pixels with relative displacement. This relative displacement depends on the variable z .

When we analyze any 3D object, we can see the light emitted by that object can be considered as the emission of point sources that emit in any direction. However, the most significant light ray for us is the optical axis direction. Once this direction is known, each ray can be described by spatial and angular coordinates regarding the optical axis [10]. If we analyze the irradiance distribution that each image records, we can observe that each pixel has its specific irradiance values [10]. In addition, it is necessary to remember that the

* Electronic address: icordool7@alumnes.ub.edu

image of a point in the object plane is not a point itself in the image plane, since the diffraction effect is produced, due to the camera aperture. Moreover, the irradiance distribution in the pixels themselves is determined by the Bessel function or Airy function. Next, we can see how each camera sensor pixel, in its central position and at certain angles, records the irradiance coming from a point of the object plane [10].

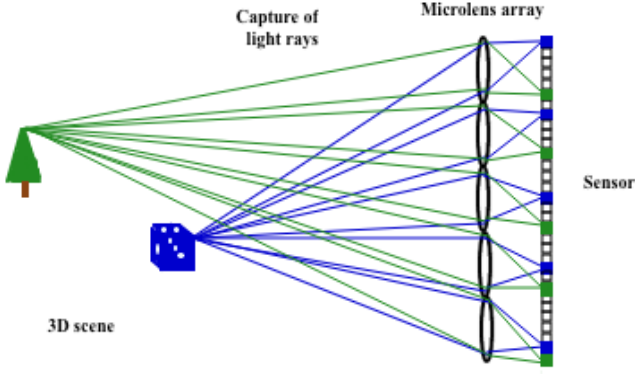


FIG 2. Integral imaging system. Each pixel collects an irradiance value at its center.

II. COMPUTATIONAL METHOD FOR THE PICKUP OF ELEMENTARY IMAGES

One of the important aspects to understand how the Integral imaging system works is the concept of pixels irradiance distribution, since it is fundamental to understand the computational reconstruction of the elementary images. Since in this study we do not work with the polarization of light, then, the equation representing the Integral imaging irradiance distribution is as follows:

$$I(x, y, z) = \sum_{k=0}^{N_x-1} \sum_{l=0}^{N_y-1} i_{k,l} \left(x - k \frac{Wpf}{c_x z}, y - l \frac{Hpf}{c_y z} \right) \quad (1)$$

In the equation (1), the term p is the relative displacement of the elementary images, the term f is the focal of the camera lens, c_x and c_y are the sensor sizes, N_x and N_y are the number of elementary images in x and y axis, respectively. W and H are the number of pixels of the elementary images ($W \times H$), and k and l are the indexation of the images N_x and N_y , respectively.

A. Pickup of elementary images

The equation (1) tells us the obtaining of an Integral imaging is the result of the average of all the elementary images displaced. In the next illustration, FIG 3, the concept of sum and average of elementary images is better represented.

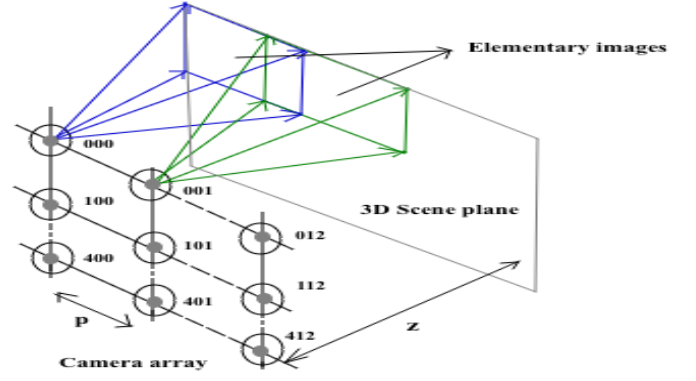


FIG 3. Pickup of the elementary images.

The 3D scene computational reconstruction allows us to visualize and select each plane that composes it since as, we can see in the equation (1), it depends on the variable z . Therefore, we can advance plane by plane the entire 3D scene in this way. Then, deductively, the set of all planes represent the volume of the 3D scene.

In order to perform the computational reconstruction of the 3D scene, we need to know a set of variables described by equation (1). The next TABLE 1 shows us the values of the different variables:

TABLE 1. Different variables values.

Elementary images	$N_x = 13; N_y = 5$
Sensor size	$c_x = 22,2 \text{ mm}; c_y = 14,8 \text{ mm}$
Focal length	$f = 18 \text{ mm}$
Camera relative displacement	$p = 5 \text{ mm}$
Scene depth range (z)	240-700 mm
Image size (WxH)	3888 x 2592 pixels

There exists two methods to capture elementary images of our 3D scene. We can work with a large focal or a small focal. Each of these methods has advantages and disadvantages, and although the 3D scene captured in this work contains a large depth (240-700 mm), we have chosen to work in near the field mode by selecting a focal length of 18 mm, as shown in TABLE 1. The reason for the choice of this mode will be discussed later.

B. Computational Reconstruction

The differences between the different points of view of a point in an object provided by the eyes, is what we call the binocular disparity, and it is the responsible of providing depth. The relative shifts of elementary images provide us different points of view of the same point; then, they simulate the disparity effect, since the emission of light from one point of an object is recorded at a different place in each elementary image.

The best way to understand the Integral imaging computational reconstruction is to comprehend how the variable z acts in equation (1), since it is responsible for the pixels' relative displacement of the elementary images in order to obtain the different 3D scene planes. This is the key point, since for each z we will obtain a concrete pixels' displacement values; then, with the computational reconstruction, each z will mark all points of the plane with a relative displacement between pixels that equals to the disparity. Thus, the computational Integral imaging obtained will be the sum and average of all those points with the same displacement.

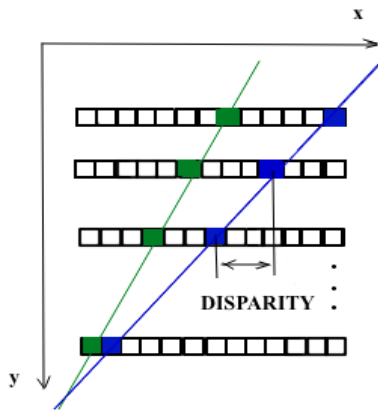


FIG 4. Different locations of the same point in elementary images. Disparity of the points.

III. EXPERIMENTAL RESULTS

In the FIG 5 we can see the proposed 3D scene for our work. This scene is illuminated as said above, by four points of natural light, two in the front and two in the right side. Next, we discuss some features and some elements of our objects.



FIG 5. Experimental 3D scene.

When we analyze the 3D scene in detail, we can see there are several objects that represent occlusions of other objects;

that is, these objects are in front of other objects and do not allow to see exactly what is behind them.

Next, we analyze all the occlusions of all the objects present in our 3D scene.

We can see the two yellow flowers between the planes of distance $z = (270-310)$ mm and $z = (360-390)$ mm cover substantially part of the black and brown trains. In the upper left, when choosing the $z = 460$ mm plane, a silver chimney becomes hidden by the tree in front of it. If we look at the back between planes $z = (500-560)$ mm, the bridge bars are hiding the blue train. On the other hand, there are also certain 3D scene angle still hidden.

As we will see later, the problems caused by occlusions presented by different objects and certain angles that are not visible are reduced or solved by horizontal and vertical parallax in the InI computational reconstruction..

A. Elementary images

Our 3D scene has a large width, so there are more elementary images taken on the horizontal axis than on the vertical axis. We have $N_x = 13$ elementary images on the x axis and $N_y = 5$ elementary images on the y axis, a total of 65 elementary images. The numbering positions of these elementary images can be represented as a matrix. Before presenting the results of the computational reconstruction, we want to display some of the elementary images of the whole set.

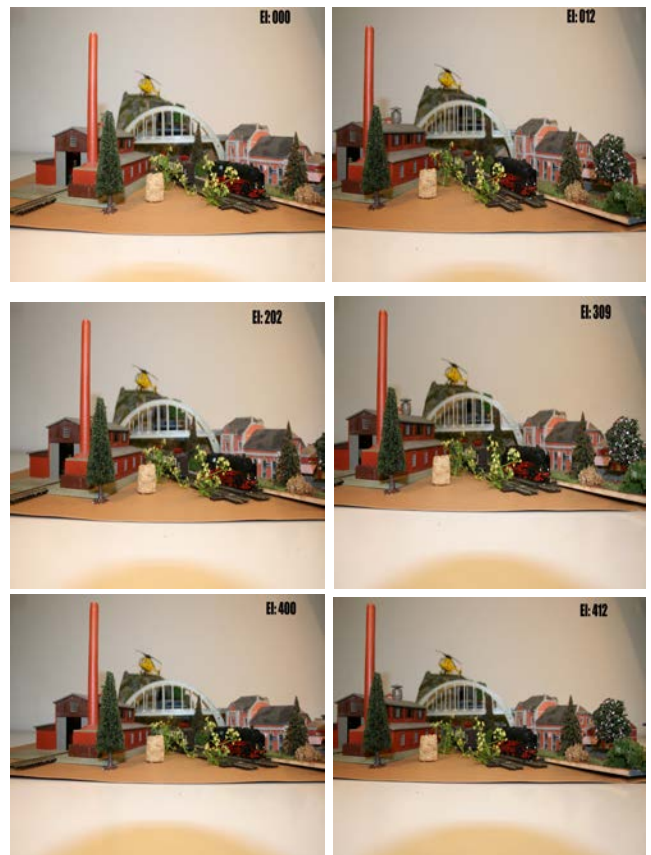


FIG 6. Six examples of elementary images.

We can appreciate that with the horizontal and vertical relative displacement of the elementary images, some of the entirely occluded objects become totally visible and some parts of some objects become visible as well. Several parts of the trains and certain angles that were not still visible in the

initial shot, are visible now. Once the computational reconstruction of the elementary images is performed, we will show the result obtained with some Integral imaging in function of the variable z .

B. Plane by plane reconstruction

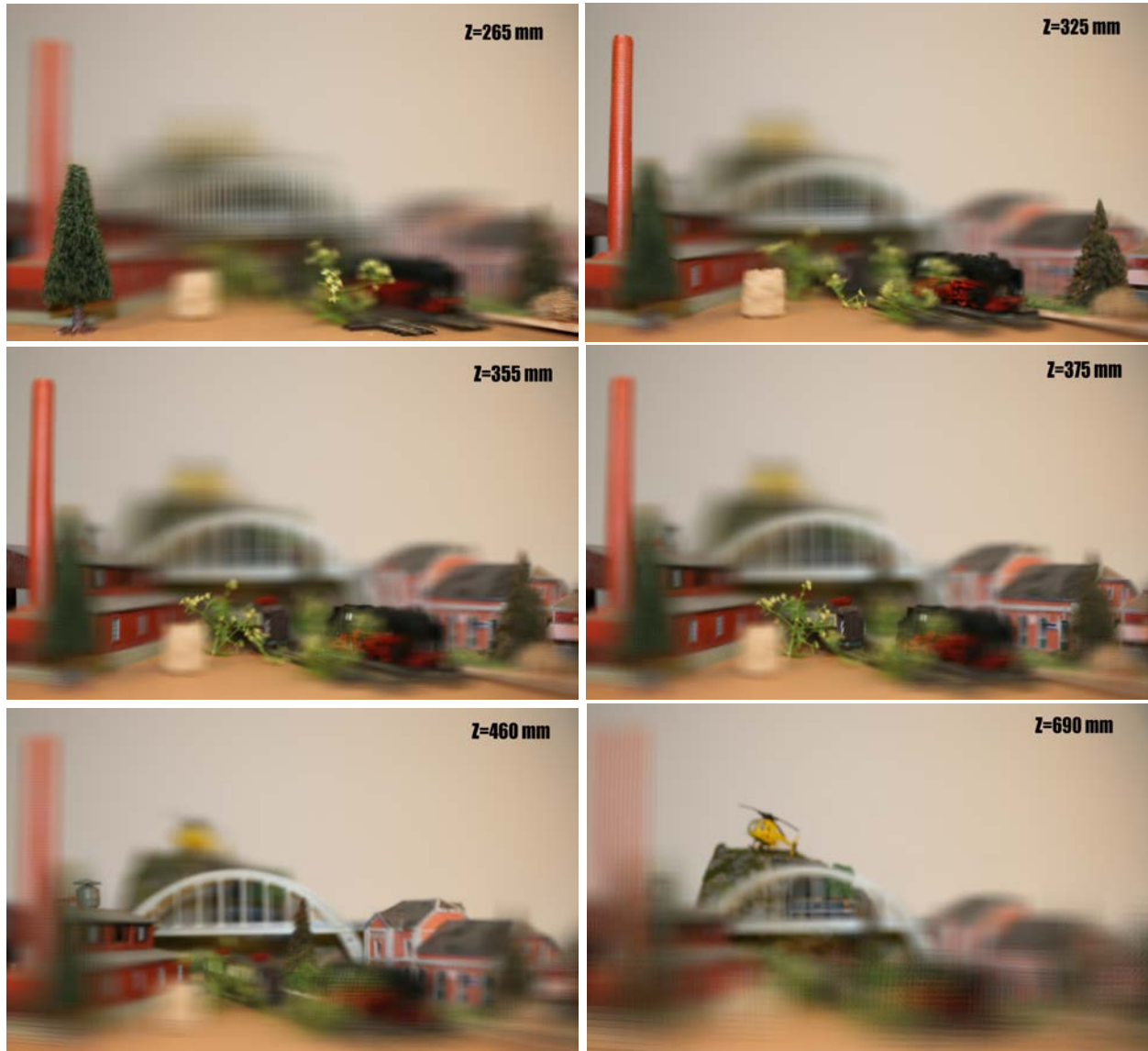


FIG 7. Experimental results. Integral imaging computational reconstruction of six planes.

In the FIG 7, we can illustrate these six significant planes, in which we can visually and analyze all the aforementioned aspects clearly. The first Integral imaging shows the plane at $z = 265$ mm, where we can see, on the left the tree perfectly defined and how the first yellow flower shows us a branch with flowers clearly defined as well. The second Integral imaging is at a distance $z = 320$ mm and, there, we can see perfectly defined in the same plane some parts like the wheels of the central part of the black train, the right tree and the red chimney on the left side. The third Integral imaging in the $z = 355$ mm plane is one of the key images, since we observe how the occlusion presented by the yellow flower in front of

the black train becomes diffuse and certain parts, that could not be visualized from the black train, become perfectly visualized now. In the fourth Integral imaging located in the $z = 370$ mm plane, we can perfectly observe the back of the brown train and, next to the train, the third yellow flower. The fifth Integral imaging in a plane of $z = 460$ mm is also one of the key images. We can see the small chimney above the roof in the upper left, a tree on the right, the last building and, finally, the whole brown train due to the third yellow flower fading. Finally, in the sixth Integral imaging, plane $z = 680$ mm, we can see how the bridge verticals bars fade so we

can see the blue train and the yellow helicopter on the top of the mountain.

We were able to visualize six of the most important computational reconstruction planes. The computational reconstruction is not limited to six planes, as said before, giving values to the variable z we can obtain different planes.

IV. CONCLUSIONS

In this work we have used a Canon EOS 400D (Rebel XTi) camera with a CMOS sensor. One of the Key decision about this work has been the choice of the focal length of the camera. The *TABLE 1* shows we have worked with a focal length of 18 mm. Although, with a longer focal length, for example 55 mm, we get more depth of field and therefore a higher resolution of the distant planes. On the other hand, with a smaller focal, we can select more distances between planes. Some of these planes have a relative separation of 5 mm, while it can not be achieved with a 55 mm focal.

As mentioned earlier, we have been able to verify the problems caused by the different occlusions have been reduced or solved by horizontal and vertical parallax, as the occlusions fade and the depth planes become perfectly observable.

Computational Integral imaging is a technique that does not require complex technologies to work, since only with a camera and a computer program can achieve good results. Even once the different planes are obtained, we know several techniques to achieve volumetric reconstruction of the 3D scene in the physical space. Even so, we have been able to verify that there are some limitations associated with this

technique, like its limitation in the vision angle and its shallow depth of field. On the other hand, high-resolution sensors are needed and the high computational power required to obtain an Integral imaging by computation is very high.

Holography and Integral imaging are the two techniques that best recreate a 3D object. Although holography is the 3D reconstruction technique that gives the best 3D feel while registering amplitude and phase of light, it is limited by the use of coherent light and mechanical stability, computational Integral imaging is also a good 3D reconstruction technique, even with some limitations.

Acknowledgments

First of all, I would like to thank my tutor (TFG), Dr. Artur Carnicer Gonzalez, for helping me when necessary and for guiding me throughout the whole project. I want to thank Dr. Santi Vallmitjana for borrowing me the camera when necessary and Dr. Salvador Bosch for helping me and advising me when I asked for it. On the other hand, I thank my family, especially my mother Adelina Oliver Cordoba, my aunt Olga Oliver Cordoba, my grandfather Domingo Oliver Arroyo for supporting me and Ester Juncà. I am grateful to some of my friends; Albert Costa Lopes, Xavier Lloret Bosch, Oriol Burkhardt Martinez, Daniel Rigat Puig, Aleix Castillo Casals and Marcel Barri Alabau for helping me and trusting me. Also, I would like to thank my friend Eva Domingo, Daniela Miklasova, for some translations and, Toni Guasch, for the language supervision of work. Finally, I want to thank Miquel Galeano for borrowing me the objects I needed to recreate the 3D scene.

References

- [1] M.G. Lippmann, "Epreuves reversibles donnant la sensation du relief," *J. Phys. (Paris)* **7**, 821-825 (1908).
- [2] M.G. Lippmann, "LA photographie integrale," *CR Acad. Sci.* **146**, 446-451 (1908).
- [3] A.Stern and B.Javidi, "3D image sensing, visualization, and processing using integral imaging", *PROCEEDINGS OF THE IEEE*, VOL. 94, NO. 3, MARCH 2006.
- [4] Xiao Xiao, Bahram Javidi, Genaro Saavedra, Michael Eismann, and Manuel Martínez-Corral, "Three- dimensional polarimetric computational Integral imaging", 2 July 2012 / Vol. 20, No. 14 / *OPTICS EXPRESS* 15481.
- [5] Sungyong Jung, Sung-Wook Min, Jae Hyeung Park, and Byoung-ho Lee, "Study of three-dimensional Display system Based on Computer-Generated Integral Photography". *Journal of the Optical Society of Korea*, Vol 5, No. 2, June 2001, pp. 43-48.
- [6] Okoshi, Takanori, *Three-dimensional imaging techniques*, ACADEMIC PRESS, INC. **2**, 12-28, London 1976.
- [7] S. H. Hong, J.S. Jang, and Bahram Javidi, "Three-dimensional volumetric object reconstruction using computational integral imaging", *Opt. Express* **12**(3) 483-491, 2004.
- [8] U. Schnars and W. Jüptner, "Direct recording of Holograms by a CCD target and numerical reconstruction," *Appl. Opt.* **33**, 179-181 (1994).
- [9] Bahram Javidi, Fumio Okano, Jung-Young Son, "Three-dimensional Imaging, Visualization, and Display". Springer (2009). **14**, 281-299.
- [10] H. Navarro, M. Martínez-Corral, A. Dorado, G. Saavedra, A. Llavador, and B.Javidi " Capture of the spatio-angular information of a 3D scene", *Opt. Pur. Apl.* **46**, 147-156 (2013).
- [11] Artur Carnicer and Bahram Javidi, "Polarimetric 3D integral imaging in photonstarved conditions", 9 Mar 2015, Vol. 23, No. 5, *OPTICS EXPRESS* 6408.